Effect of laser pulse shape and duration on spectrum width of coherent LIDAR

Zhichao Bu (步志超), Siying Chen (陈思颖)*, Yinchao Zhang (张寅超),
He Chen (陈 和), Xianying Ge (葛宪莹), and Pan Guo (郭 磐)

Beijing Institute of Technology, Beijing 100081 China
*Corresponding author: csy@bit.edu.cn

Doppler spectrum width, which relates to wind turbulence, is one of the essential parameters of coherent LIDAR. Using the Fourier transform theorem and the definition of correlation function, the power spectrum function in the stationary condition is deduced. The effects of pulse shape, pulse duration and the windowing are included. The spectrum width resulted from the turbulence is given under Kolmogorov turbulence model. Based on the power spectrum theory, the spectrum broadening by different pulse shapes and pulse durations are calculated. To validate the accuracy of the theory and usage in the retrieval of turbulence parameters, the numerical simulations of the echo signal are carried out in turbulence conditions. The statistics characteristics of the spectrum broadening from laser pulse shapes and durations are inverted and compared. The results show that the spectrum broadening varies greatly due to the selection of pulse shapes and pulse durations, and the numerical simulation is in accordance with the theory results.

OCIS codes: 280.3640, 070.4790, 010.1330, 170.3340.
doi: 10.3788/COL201412.S12801.

The data of wind LIDAR measurements can be used for retrieval of wind turbulence parameters[1–4], such as the dissipation rate of the turbulent energy, the variance of the wind velocity and the outer scale of turbulence. Several estimation methods of turbulence parameters are known for coherent Doppler LIDAR, and Doppler spectrum width[2–4] is one of the most important methods.

However, the accuracy of spectrum width method may suffer from two problems. First, there is an extra spectrum width caused by the laser pulse shape. Second, the windowing effect on signal processing leads to the spectrum width broadening. V. A. Banakh[3] gave the theory expression of spectrum width with the turbulence energy dissipation rate (TEDR) in Gaussian pulse shape. Frehlich[4] had shown the spectrum widen by the widowing effect under ideal Gaussian conditions. Nonetheless, the Gaussian pulse shape is not the only laser pulse shape used for coherent Doppler LIDAR, but the pulse shapes of the Lorentz[5], Rectangular[6] and Hyperbolic secant[7] were reported and also the durations of the pulse are not infinite. To my knowledge, the effect of laser pulse shape and pulse duration on spectrum width of coherent LIDAR has not been systematically elaborated in the literatures.

In this present paper, the power spectrum function in stationary conditions is deduced under the Fourier Transform theorem and the correlation definition of function in Section 2. Based on the power spectrum expression, the spectrum broadening due to laser pulse shapes and pulse durations are calculated in Section 3. To validate the accuracy and practicability of the theory, numerical simulations of the echo signal are carried out under turbulence conditions, the relative errors of the spectrum width are retrieved in section 4, and the statistics results show good accordance with the theoretical values. Results of the present work will contribute to the improvement of the accuracy in the retrieval of the turbulence parameters, especially in the case of weak turbulence.

The spectrum width due to the laser pulse and windowing effect is independent of the turbulence. In this section, the theory of the spectrum width is discussed in stationary circumstance.

The signal of coherent Doppler LIDAR is a random process and suited to be estimated by spectrum estimation. The most fundamental spectrum estimate theory is the periodogram, which is defined as[8]

$$\hat{P}_u(nF) = \frac{1}{M}\left|\sum_{m=0}^{M-1}\omega(mT_s)\right.$$
$$\left. S(mT_s)\times\exp(-2\pi imn/M)\right|^2, \qquad (1)$$

where $S(mT_s)$ denotes the echo signal, m is the data index and T_s refers to the sampling interval of the data, $\omega(mT_s)$ is the windowing function, and M is the sampling number within a range gate.

Based on the Fourier transform theorem and the definition of the correlation function, Eq. (1) can be rewritten as

$$\hat{P}_u(nF) = \frac{1}{M}\left|\sum_{m=0}^{M-1}\omega_{win}(mT_s)S(mT_s)\times\exp(-2\pi imn/M)\right|^2$$

$$= \frac{1}{M}\left|\sum_{m=0}^{M-1}\omega_{win}(mT_s)\times\exp(-2\pi imn/M)\right|^2$$

$$\otimes\left|\sum_{m=0}^{M-1}S(mT_s)\times\exp(-2\pi imn/M)\right|^2$$

$$= \left|\sum_{k=0}^{M-1}\omega_{win}(kT_s)\times\exp(-2\pi ikn/M)\right|^2$$

$$\otimes\sum_{m=-(M-1)}^{M-1}\left[\frac{1}{M}\sum_{n=0}^{M-1-m}S(kT_S)S(k+m)T_S\right]$$
$$\exp(-2\pi imn/M)$$

$$= \left| F(\omega_{win}(mT_s)) \right|^2 \otimes \sum_{q=-(M-1)}^{M-1} \hat{R}_S(q) \exp(-2\pi iqn/M), \quad (2)$$

where $F(\omega_{win}(mT_s))$ is the Fourier transform of $\omega_{win}(mT_s)$, and $\hat{R}_S(q)$ denotes the estimation of the covariance of the signal, which can be expressed as[9]

$$\hat{R}_S(\tau) = SNR \times \exp(2\pi if\tau)$$
$$\int_{-\infty}^{+\infty} \omega_{tpulse}(t)A_L(t)\omega_{tpulse}^{*}(t)A_L^{*}(t-\tau)dt, \quad (3)$$

where SNR is signal to noise rate, A_L represents for the amplitude distribution of the pulse shape, and ω_{tpulse} is the pulse duration function.

Thus, the power spectrum can be represent as

$$\hat{P}_u(nF) = SNR^2 \times \left| F(\omega_{win}(mT_s)) \right|^2$$
$$\otimes \left| F(\omega_{tpulse}(mT_s)) \otimes F(A_L(mT_s)) \right|^2. \quad (4)$$

Eq. (4) gives the relationship between the power spectra and the convolution of the widowing function, laser pulse shape and pulse duration under stationary conditions. Once the power spectrum is deduced, the spectrum width can also be calculated through the secondary moment of the power spectrum.

$$\hat{\sigma}^2 = \overline{P}_u \sum_{k=k_m-k_1}^{k_m+k_2} \left[\Delta fk - \hat{f}_D \right]^2 \hat{P}_u(nF), \quad (5)$$

where $\hat{\sigma}$ is the width of the power spectrum, Δf is the frequency bin width, $\hat{f}_D$ is the mean frequency, k_1 and k_2 are the numbers of spectral channels left (right) from the channel k_m at the spectrum estimate maximum, and $\overline{P}_u$ is the normalized signal power of the power spectrum.

Considering the effect of wind turbulence, the width of the power spectrum (in the velocity space) can be expressed as[4]

$$\left\langle \hat{\sigma}^2 \right\rangle = \sigma_{win}^2 + \sigma_{laser}^2 + \sigma_{turb}^2, \quad (6)$$

where σ_{win} is the basic spectrum width related to the windowing effect, which is the spectral leakage when the signal is confined to a few spectral bins, and this term can be calculated through the spectrum width of the constant echo signal, σ_{laser} is the spectrum width induced by the laser pulse shape and pulse duration, and σ_{turb} is the term related to the spectrum broadening resulting from the turbulence.

For the Kolmogorov turbulence model, σ_{turb} can be written as [9]

$$\sigma_{turb} = \sqrt{\frac{9}{40} C_v} \varepsilon^{1/3} \Delta L^{1/3}, \quad (7)$$

where C_v is a constant, ε is represent for TEDR, and ΔL is the range gate of lidar signal.

The normalized intensity mathematical expressions of the mentioned pulse shapes in introduction can be written as per the following:

$$p(t) = \begin{cases} \dfrac{2\sqrt{\ln 2}}{\sqrt{\pi}tpulse} \\ \times \exp\left\{ -\left(2\sqrt{\ln 2}\,\dfrac{t}{tpulse}\right)^2 \right\} & Gaussian \\[2em] \dfrac{2}{\pi tpulse} \times \dfrac{1}{1+\left(\dfrac{2t}{tpulse}\right)^2} & Lorentzian \\[2em] \dfrac{\ln(\sqrt{2}+1)}{tpulse} \\ \times \sec h^2\left(2\sqrt{\ln 2}\,\dfrac{t}{tpulse}\right) & Hyperbolic - \sec ant \\[1em] rect(-tpulse/2, tpulse/2) & Rectangular. \end{cases}$$
$$(8)$$

where tpulse is the pulse width, which is defined by the full width at half maximum (FWHM) of the maximal intensity, and rect is the rectangular function.

According to Eq. (4), the power spectrum of the above pulse shapes with infinite duration can be expressed as

$$p(\omega) = \begin{cases} \dfrac{tpulse}{2\sqrt{\pi \ln 2}} \exp\left[-tpulse^2\,\dfrac{\omega^2}{4\ln 2} \right] & Gaussian \\[1.5em] \dfrac{1}{\pi^2}tpusle \\ \times \left[BesselK[0, \dfrac{tpulse \times abs[\omega]}{2}] \right]^2 & Lorentizian \\[1.5em] \dfrac{\ln(\sqrt{2}+1)\pi tpulse}{8\ln 2} \\ Sech^2[\pi \dfrac{tpulse}{4\sqrt{\ln 2}}\omega] & Hyperbolic - \sec ant \\[1.5em] \dfrac{tpulse^2 \times \sin c^2(\dfrac{tpulse \times \omega}{2})}{2\pi} & Rectangular. \end{cases} \quad (9)$$

Based on Eq. (9), the pulse shapes with a pulse width of 400 ns are shown in Fig. 1, and the corresponding power spectrum with an infinity pulse duration are illustrated in Fig. 2.

As shown in Fig. 1 and Fig. 2, with the same pulse width, the power spectra of different pulse shapes vary greatly. The spectrum widths, which can be calculated through Eq. (5), are thus a lot different from pulse shapes. The Lorentz pulse shape has the smallest pulse width, and the Rectangular shape has the biggest pulse width. However, the true pulse duration cannot be infinite, and the influence of the pulse duration should be considered according to Eq. (4). The power spectrum can be calculated through the convolution operation between the pulse power spectrum and the pulse duration spectrum function.

In order to compare this spectrum width more directly, the values of the width are calculated through the second moment of the power spectrum, and the relative width bias can be introduced as
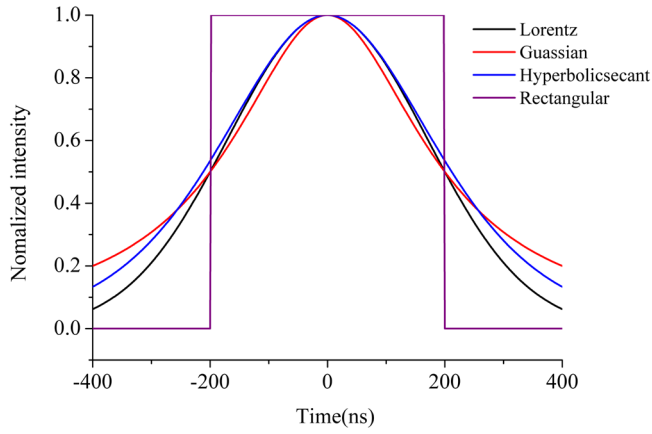
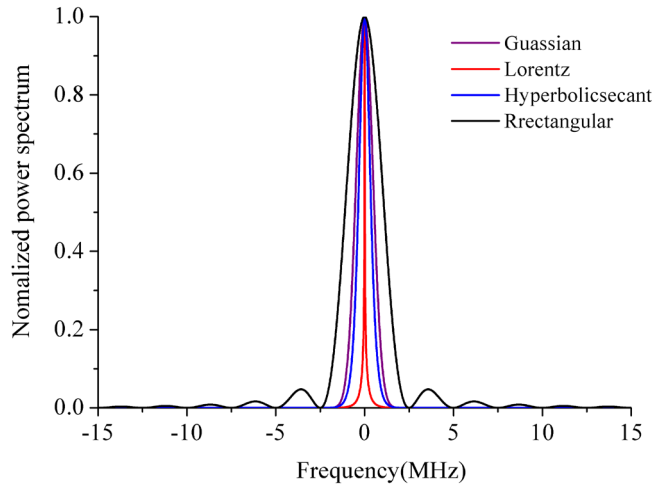Fig. 1. Illustration of the normalized intensity of the mentioned pulse shapes.

Fig. 2. Illustration of the corresponding power spectrum of different pulse shapes.

$$b = (w/w_g - 1) \times 100\%, \qquad (10)$$

where w is the pulse width of different power spectrum and w_g is the pulse width of the Gaussian pulse with infinite pulse duration.

Choosing different pulse durations of the given pulse shapes, we can derive the pulse width of the power spectrum as shown in Table 1, and the relative width bias is also include. The '×' in Table 1 represents for magnification of the pulse width.

From Table 1, we can see that the spectrum widths vary greatly from different pulse durations and pulse shapes, with the greatest relative bias of 699.4%. The two times of pulse width is the most comparability set of data, the relative width bias changes from 114% to 670.1%, which is used in the following Section. Thus, only using Gaussian shape and ideal pulse duration for spectrum broadening will make the results of TEDR incredible, especially in the case of weak turbulent.

In order to validate the accuracy, especially to validate the usage of the theory in the turbulence conditions, the numerical simulations are carried out. Using the feuilleté model[10], the time domain signal is simulated under non-stationary atmospheric conditions. The area of the laser propagation in space by the pulse $P_T(t)$ is divided into n_L layers, and the signal received at one time is a sum of the contributions from all these layers. The signal can be written as follows:

$$S(mT_S) = \left[\frac{SNR}{2\sum_0^{n_L} P_T(dk)} \right]^{1/2} \sum_{k=0}^{N} a(k+m)P_T^{1/2}(dk)$$

$$\times \exp\left\{ -j\frac{4\pi}{\lambda} mT_s V_r \left[d(k+m) \right] \right\} + \frac{1}{\sqrt{2}} n_m, \quad (11)$$

where m is the number of the sampling, a_k and n_m are independent complex Gaussian random numbers, and V_r are the real random values of wind field, including the random velocity caused by turbulence[9,11] and the modulation frequency by AOM.

The simulation conditions used in this paper are summarized in Table 2. The parameters shown in the table are typical values used for coherent Doppler LIDAR systems, and the pulse width is the same as in Section 2.

According to Eq. (1) and Eq. (11), the power spectrum can be obtained from 180 m to 3000 m with the range gate of 60 m. Taking the fourth range gate as the object to study, 300 independent shots are used for the spectrum accumulation. After noise elimination and averaging, the whole spectrum width $\hat{\sigma}$ and σ_{win} can be calculated. Given the TEDR value in Table 2, one can estimate the

Table 1. The relative width bias of different pulse shapes and pulse durations

Pulse types	Infinity	4 ×	3 ×	2 ×	1 ×
Lorentzian width (MHz)	0.24898	1.043	1.2416	1.6857	2.9448
Lorentzian bias	46.8%	122.6%	165%	259.8%	528.5%
Gaussian width (MHz)	0.46848	0.47145	0.49541	1.0028	2.8404
Gaussian bias	0	6.3%	5.7%	114%	507%
Hyperbolic width (MHz)	0.38694	0.66177	0.93296	1.2994	2.9105
Hyperbolic bias	16.8%	41.2%	99.1%	177.4%	521.2%
Rectangular width (MHz)	0.64456	3.6067	3.5959	3.6080	3.7219
Rectangular bias	37.8%	669.8%	667.5%	670.1%	699.4%

Table 2. Simulation conditions

Parameter	Value
Laser wavelength(μm)	2
Laser energy(j)	0.1
Pulse FWHM(ns)	400
The thick of the slice(m)	0.3
Range gate(m)	60
Sample rate(MHz)	500
Backscatter coefficient of aerosol($m^{-1}sr^{-1}$)	8×10^{-8}
Transmittance	0.8
System efficiency	0.015
the modulation frequency of AOM(MHz)	100
TEDR(m^2/s^{-3})	5×10^{-2}

Table 3. The evaluation of the pulse width and the corresponding error

Pulse type	Mean (MHz)	var (MHz)	Err
Guassian	1.0335	5.9e-3	3.06%
Lorentz	1.6721	1.31e-2	0.83%
Hyperbolic scecant	1.335	9.5e-3	2.53%
Rectangular	3.6993	5.81e-2	2.53%

statistical of the spectrum broadening $\hat{w}$ by laser pulse shape and width according to Eq. (6) and Eq. (7).

The two times of the pulse width of the pulse shapes was chosen. The statistical spectrum width results of different pulse shapes from 300 independent shots are illustrated in Fig. 3.

One can see that the distribution of the histograms is an approximate Gaussian distribution. The statistics results of the mean values and variance (*var*) are presented in Table 3, and the error of spectrum width estimation in Table 3 are calculated through the estimate error function, defined as

$$Err = \left[\left\langle \left(\hat{w}/w - 1 \right)^2 \right\rangle \right]^{1/2} \times 100\%, \qquad (12)$$
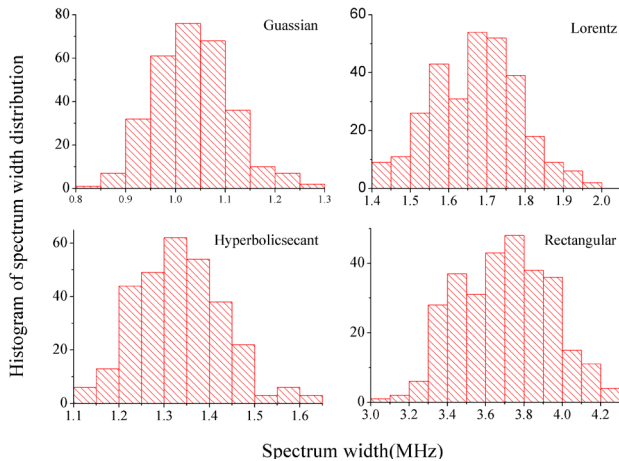
where w is the theoretical calculation result of the power spectrum width.

From Table 3, it can be seen that the error of the spectrum width estimation is smaller than 3.06% for different pulse shapes with the two times of the pulse width. We can draw the conclusion that the numerical simulation is in accordance with the theory results quiet well, which can further validate the usage of the theory in the turbulence conditions.

Effect of different pulse shapes and pulse durations on the spectrum width of coherent Doppler LIDAR is analyzed. The power spectrum function in stationary conditions is deduced. The results show that the spectrum broadening varies greatly due to different selection of pulse shapes and pulse durations. To validate the accuracy of the theory, the numerical simulations of the echo signal are carried out in turbulence conditions. The estimate error between the simulation and theory is less than 3.06% in non-stationary conditions.

Fig. 3. The histograms of simulated spectrum width by different laser pulse shapes

References

1. V. A. Banakh and C. Werner, Proc. SPIE **5575,** 55 (2004).
2. S. Kameyama, T. Ando, K. Asaka, Y. Hirano, and S. Wadaka, Geoscience and Remote Sensing, IEEE Transactions. **47,** 3560 (2009).
3. S. Brousmiche, L. Bricteux, P. Sobieski, B. Macq, and G. Winckelmans, in *Proceedings of IEEE Conference on Geosciences and Remote Sensing Symposium* **2783,** (2007).
4. R. Frehlich, and L. Cornman, Appl. Optics **38,** 7456 (1999).
5. Y. Liu, J. Liu, and W. Chen, Chin. Opt. Lett. **9,** 090604 (2011).
6. R. T. Menzies, M. J. Kavaya, P. H. Flamant, and D. A. Haner, Appl. Optics **23,** 2510 (1984).
7. Y. Hao, Q. Ye, Z. Pan, H. Cai, and R. Qu, Optik **16,** 124 (2012).
8. R. Frehlich, J Atmos. Oceanic Technol. **13,** 646 (1996).
9. R. Frehlich, J Atmos. Oceanic Technol. **14,** 54 (1997).
10. P. Salamitou, A. Dabas, and P. H. Flamant, Appl. Optics **34,** 499 (1995).
11. A. M. Dabas, P. Drobinski, and P. H. Flamant, J Atmos. Oceanic Technol. **17,** 1189 (2000).